Microdosimetry of Very-High-Energy Heavy Ion Beams for Electronics Testing Using Silicon-on-Insulator Detectors

Andreas Waets, Natalia Emriskova, Ruben Garcia Alia, *Member, IEEE*, Karolina Klimek, Vladimir Pan, Anatoly Rosenfeld, *Life Senior Member, IEEE*, Linh T. Tran, *Member, IEEE*, James Vohradsky, Angela Kok, Marco Povoli, Petteri Nieminen, and Uwe Schneider

***Abstract*— This article explores the use of microdosimetry with a silicon-on-insulator (SOI) detector for characterizing very-high-energy (VHE) heavy ion beams used specifically for single event effect (SEE) testing of electronics. The detector was deployed at CERN's heavy ion facility for radiation effects testing and exposed to lead ion beams in the 100–1000 MeV per nucleon kinetic energy range. The implications and possible benefits of using microdosimetry for SEE testing purposes are discussed.**

***Index Terms*— CERN, FLUKA, linear energy transfer (LET), microdosimeter, Monte Carlo simulations, silicon-on-insulator (SOI) technology, single event effects (SEEs), very-high-energy (VHE) heavy ions.**

I. Introduction

SPACE mission success can be severely impacted by single event effects (SEEs) which are triggered when an energetic particle deposits a sufficient amount of energy in the sensitive (sub-)volume of a component. The on-board electronics on spacecraft are continuously subject to the galactic cosmic ray (GCR) spectrum which contains high energy, high charge heavy ions. Ground-based facilities are used to mimic SEE rates in orbit before implementation on a space mission by testing the components using particle beams extracted from accelerators. The SEE response of an electronic component under test is determined as a function of the linear energy transfer (LET) which is the key metric of deposited energy within the sensitive volume (SV). Radiation hardness assurance is key in space mission risk management and requires particle beams with a high LET. The use of very-high-energy (VHE) heavy ion beams [1], [2] has attracted great interest within the radiation effects testing community in recent years, due to their combination of high LET and large penetration depth in modern microelectronic components with a complex layered or 3-D structure. CERN is currently developing the capability to provide these beams for electronics testing [3]. The dosimetry of high-energy heavy ion beams presents a challenge: the particle's energetic nature makes inevitable inelastic interactions with any present in-beam equipment, generating a mixed field of both primary and secondary particles (including heavy ion fragments) at the test location [4]; energy straggling further complicates the prediction of the deposited energy in the device-under-test (DUT). Reaching particle LETs interesting for radiation hardness assurance applications (> 40 MeV $\cdot$ cm^2/mg in silicon) involves using beams at the lower edge of the VHE ion range (lower than 100 MeV/n). This can be done with a pristine beam prepared at the appropriate energy or can be achieved using passive beam energy degraders. However, also the use of degraders broadens the beam energy distribution due to energy straggling and contaminates the primary beam with fragments. As a result, the characterization of the beam in terms of the LET as a single-valued quantity becomes incomplete. SVs in modern electronic components are currently submicrometers or even nanometers in size. At these scales, energy deposition fluctuations cannot be accurately described with macroscopic mean values like the LET but rather by its stochastic, microdosimetric analog lineal energy. Microdosimetry was developed to study the effect of imparted energy on a cellular level and is generally applied in a radiobiological context [5]: the biological effectiveness of two types of radiation can be different even though they might have the same LET [6]. The LET metric is generally used in the mm–cm scale for deterministic events, whereas for microelectronics, it is more appropriate to use microdosimetry for describing stochastic events such as SEEs [7]. The LET is a deterministic, track-averaged quantity, specifying the energy loss of a particle through electronic collisions. Generally, the distinction between "unrestricted" and "restricted" LET needs

Received 12 December 2024; revised 28 January 2025 and 4 February 2025; accepted 7 February 2025. Date of publication 12 March 2025; date of current version 18 August 2025. This work was supported by the High Energy Accelerators for Radiation Testing and Shielding (HEARTS) Project, funded by the European Union through the Space Work Program of the European Commission under Grant 101082402. *(Corresponding author: Andreas Waets.)*

Andreas Waets is with CERN, CH-1211 Geneva, Switzerland, and also with the Physik-Institut, Medical Physics and Radiation Research, University of Zürich, CH-8006 Zürich, Switzerland (e-mail: andreas.waets@cern.ch).

Natalia Emriskova, Ruben Garcia Alia, and Karolina Klimek are with CERN, CH-1211 Geneva, Switzerland.

Vladimir Pan, Anatoly Rosenfeld, Linh T. Tran, and James Vohradsky are with the Centre for Medical Radiation Physics, University of Wollongong, Wollongong, NSW 2522, Australia.

Angela Kok and Marco Povoli are with SINTEF, 0314 Oslo, Norway.

Petteri Nieminen is with European Space Agency, 2201 AZ Noordwijk, The Netherlands.

Uwe Schneider is with the Physik-Institut, Medical Physics and Radiation Research, University of Zürich, CH-8006 Zürich, Switzerland.

Color versions of one or more figures in this article are available at https://doi.org/10.1109/TNS.2025.3550471.

Digital Object Identifier 10.1109/TNS.2025.3550471

© 2025 The Authors. This work is licensed under a Creative Commons Attribution 4.0 License.
For more information, see https://creativecommons.org/licenses/by/4.0/

to be made where the former includes all energy loss but the latter excludes delta rays above a certain energy threshold. The microdosimetric lineal energy is agnostic to this arbitrary limit and considers the actual deposited energy within a well-defined, micrometric volume on an event-by-event basis. The comparable SV size in microelectronics devices to the size of biological cells motivated the use of microdosimeters for radiation effects studies in microelectronics [8], [9], [10]. A key advantage in the microdosimetric characterization of a radiation field is its sensitivity to track the structure of both primary high-energy heavy ions and their secondary particles which can have different radiation quality, also taking into account secondary delta ray electrons, particle path curvature, and energy straggling. Heavy ion beam dosimetry requires simulations to determine the surface LET in silicon at the DUT, such that for each LET point, the experimental SEE cross section of a device can be obtained. The use of simulations to calculate the LET can be benchmarked by the match between simulated and experimentally obtained energy deposition spectra in a macroscopic (several 100 μm thickness) SV such as a silicon diode. In the scope of CERN's heavy ion activity, this approach was demonstrated using U beams and FLUKA [11], [12] Monte Carlo simulations at gesellschaft für Schwerionenforschung (GSI) [13]. The exact same method was applied to the Pb beam and degrader configurations used at CERN which correspond to the exact same experimental conditions to which the microdosimeter in this study was exposed. A full account of the characterization of these beams with passive degraders at CERN, including experimental silicon diode data, is given in [14]. The simulated LET values which are a result of this study will be used to compare the LET values obtained from the microdosimetry measurements. Microdosimetry offers a more direct, experimental determination of the deposited energy distribution due to VHE heavy ion beams in a micrometric volume without performing the necessary simulations that are required to extract the beam LET. The use of a silicon-on-insulator (SOI) microdosimeter also offers the advantage of measuring deposited energy in silicon, a primary material constituent of electronic components [15], [16]. For reference, in silicon, 1 MeV $\cdot$ cm^2/mg is equal to 233 keV/μm. This article is structured as follows: in Section II, the microdosimetric quantities used in this study are introduced. Section III describes CERN's infrastructure for VHE heavy ion testing of electronics and the microdosimeter test setup, followed by an overview of the measurement results in Section IV. The implications of the results for SEE testing are discussed in Section V followed by a conclusion and outlook in Section VI.

II. Microdosimetry Concepts

In microdosimetry, the deterministic, macroscopic LET is replaced by its stochastic analog the lineal energy y, defined as the ratio of energy ϵ imparted to a well-defined volume due to a single event and the ratio of the mean chord length $\bar{l}$ of the volume [17]

$$y = \frac{\epsilon}{\bar{l}}. \quad (1)$$

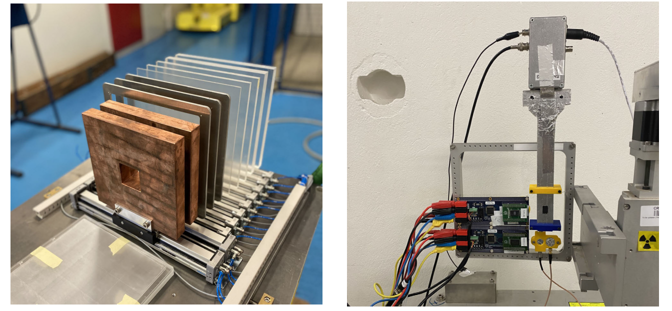

Fig. 1. LET booster system (left) comprised of a set of passive degrader plates and the DUT frame (right) with the microdosimeter, along with other devices tested in parallel.

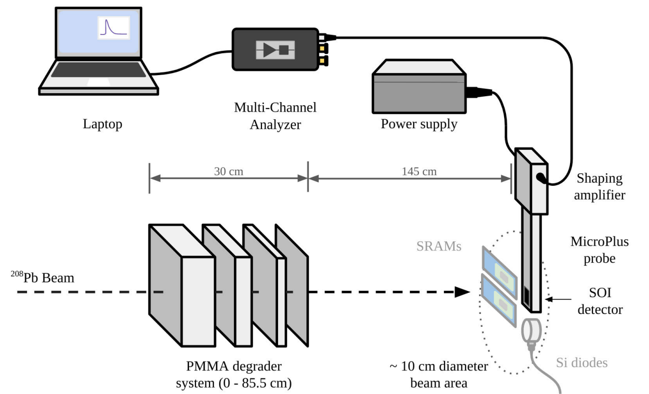

Fig. 2. Schematic of the experimental setup, showing the different components and their relative distances. The data acquisition chain shown on top was placed directly next to the test setup inside the CHARM facility.

The volume itself is more representative of the SV size in a microelectronic component than a macroscopic diode. Microdosimetric spectra are often expressed as a function of the lineal energy frequency distribution $f(y)$ and the mean of this distribution, that is, the frequency mean lineal energy $\bar{y}_F$

$$\bar{y}_F = \int_0^\infty y f(y) dy. \quad (2)$$

To reflect that higher lineal energies deposited a higher dose also the dose distribution $d(y)$ is considered, related to the frequency distribution as

$$d(y) = \frac{y f(y)}{\bar{y}_F}. \quad (3)$$

The microdosimetric lineal energy spectra are generally plotted in terms of $yf(y)$ or $yd(y)$ as a log–linear plot such that the area under the curve delimited by two values of y to the fraction of events or fraction of dose for $f(y)$ or $d(y)$, respectively [18]. The dose mean lineal energy $\bar{y}_D$ is then defined as

$$\bar{y}_D = \frac{1}{\bar{y}_F} \int_0^\infty y^2 f(y) dy \quad (4)$$

meaning that $\bar{y}_F$ is the first moment of the frequency distribution and $\bar{y}_D$ is the ratio of the second and first moment of the frequency distribution $f(y)$ [19].

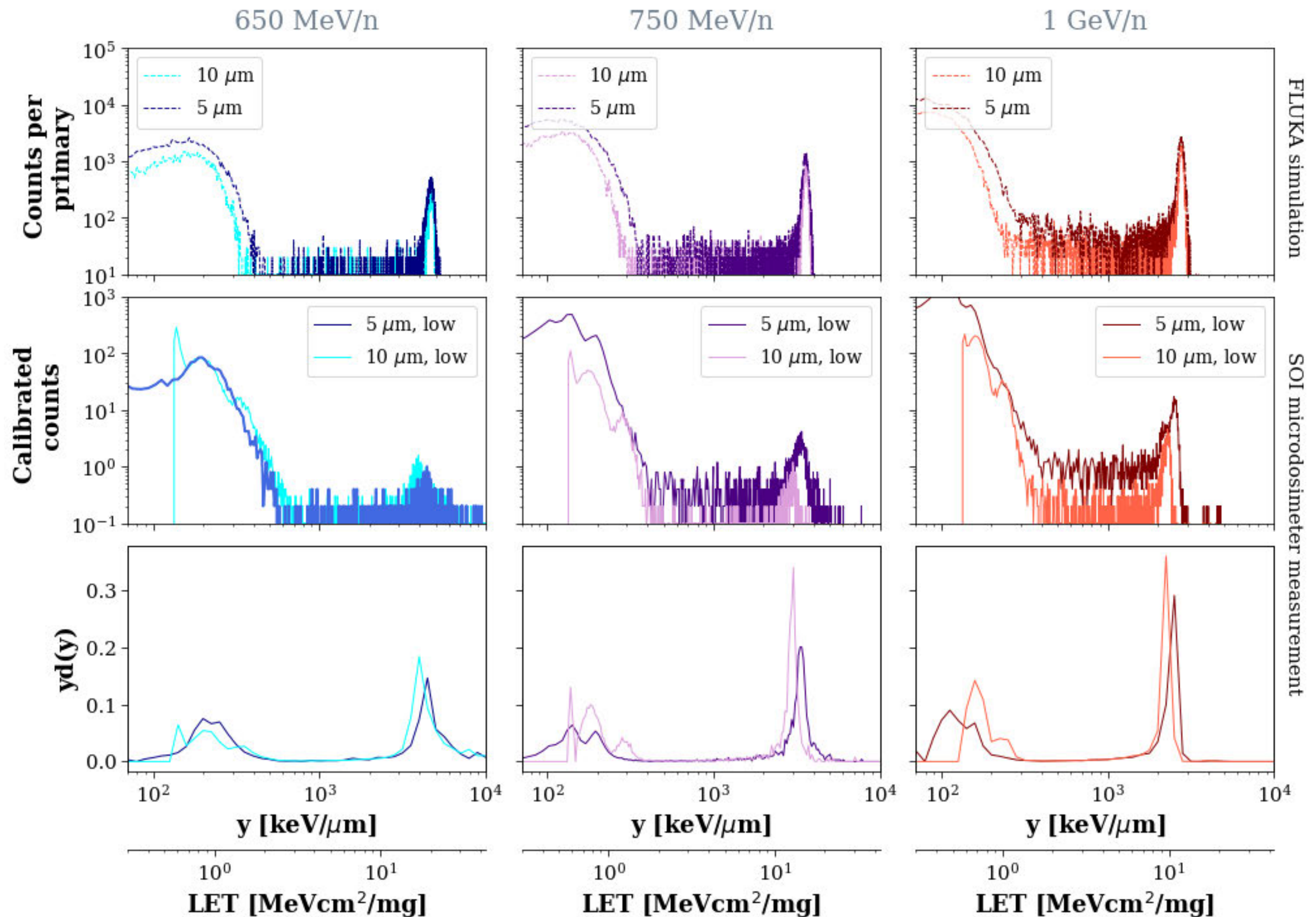

Fig. 3. Overview of the microdosimetric spectra obtained through FLUKA MC simulations (top row), measurements (middle row), and measurements when converted to a microdosimetric lineal energy spectrum (bottom row) as a function of the three standard primary energies (extracted from the CERN PS) during the test. Data are shown for both the 5 and 10 μm devices. The quoted energies denote the extraction beam kinetic energy. The conversion from lineal energy y to LET is made by equating 1 MeV $\cdot$ cm^2/mg to 233 keV/μm in silicon.

III. CERN SEE Testing Infrastructure

A. CERN Accelerator Complex and CHARM Facility

From the source, lower-rigidity ions (54+ charge state) were pre-accelerated into Linac 3 and bunched in the low energy ion ring (LEIR) before injection into the proton synchrotron (PS). Once accelerated to the desired energy (650, 750, or 1000 MeV/n in the case of the results presented in this work), the ions were slowly extracted [20] and transported through the T8 beam line in the PS East Area, down to the CERN High Energy Accelerator Mixed Field (CHARM) [21] facility where the experiments were carried out. Non-vacuum material present in the beam path (5.5 g/cm^2) degrades the centroid beam energy to 223, 361, and 660 MeV/n, respectively, calculated through Monte Carlo simulations in FLUKA [2]. Along the beamline, beam monitors provided real-time flux and beam profile information during the tests. Inside the CHARM facility directly upstream of the test station, a table with a set of movable polymethyl methacrylate (PMMA) plates (thicknesses between 0.5 and 40 mm) was placed to degrade the beam energy and thus increase the LET in fixed steps as shown in Fig. 1. The material budget due to the degraders could be varied between 0 and 100 g/cm^2. The system was designed to fully scan the Bragg peak of Pb ion beams below 1 GeV/n, that is, the maximum cumulative thickness of the degrader system is larger than the range of 1 GeV/n Pb ions in PMMA.

B. FLUKA Simulations

As already mentioned above, the T8 beam line has been fully characterized through monte carlo (MC) simulations [22] using the FLUKA code [11], [12] which is regularly used in accelerator environments and is extensively benchmarked on a microscopic level [23], [24]. Beam properties were calculated just upstream of the LET booster system and subsequently used as particle source in a highly simplified model used to probe the detector response. In this second step of the simulation, particles are propagated only through LET booster PMMA degraders, 1.5 m of air, and an SOI microdosimeter model containing 1000 silicon SVs behind a 0.5 mm PMMA sheath window, closely resembling the schematic shown in Fig. 2. The simulation physics settings included full ion transport, accounting for spallation processes such

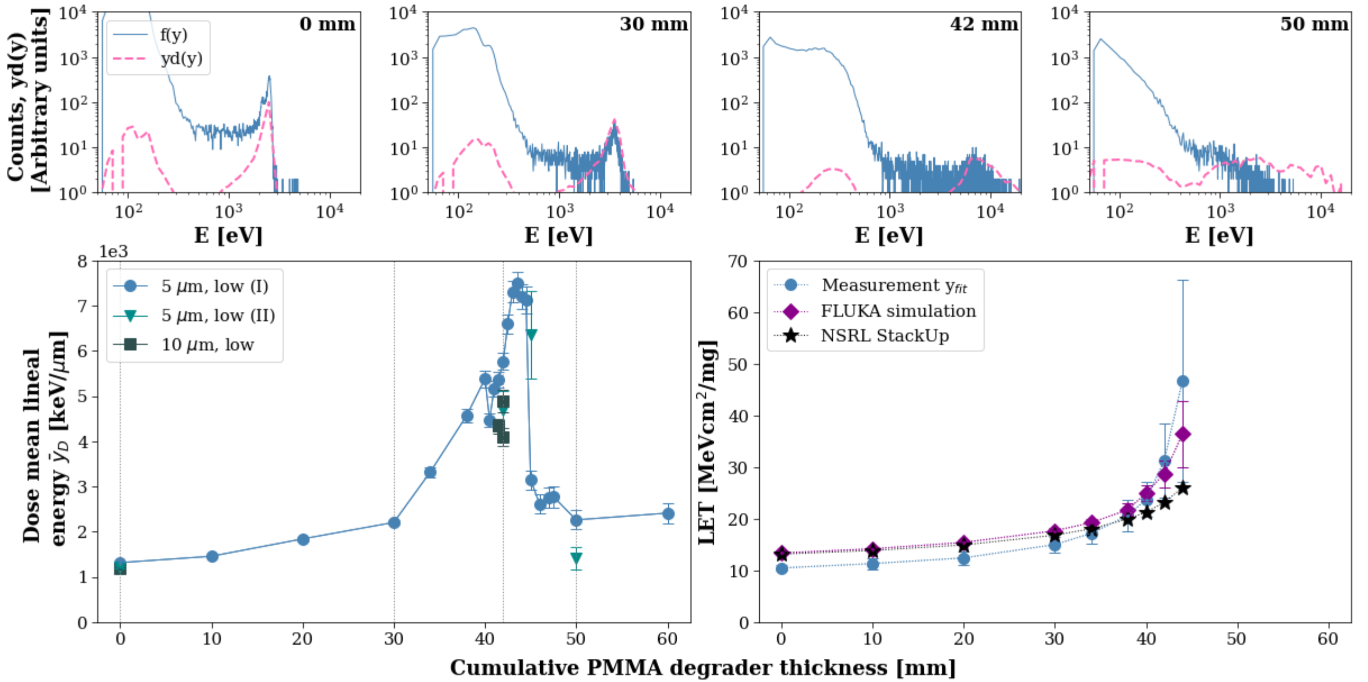

Fig. 4. Profile of the dose mean lineal energy $\bar{y}_D$ (bottom left) measured by the 5 μm device at a low gain as a function of PMMA degrader thickness starting from an extracted beam energy of 1 GeV/n (i.e., 660 MeV/n at the test location). For four thicknesses (0, 30, 42, and 50 mm), the top plots show the energy deposition and microdosimetric $yd(y)$ spectrum. The bottom right plot shows the comparison between the fit average $\bar{y}_{\text{fit}}$ values converted to LET in silicon, the LET values extracted from FLUKA simulations and the LET values obtained using the SRIM-based NSRL StackUp tool.

as fission and fragmentation, which can result from inelastic interactions of the primary beam with any material [25], [26]. To account for the accurate transport of secondary delta ray electrons emerging from ion tracks, the electromagnetic sector processes were enabled down to 150 keV. The energy deposition was recorded on an event-by-event basis in all SVs simultaneously which resulted in the spectra shown in Fig. 3 (top). Similar simulation studies have been carried out to calculate the LET at the detector position [2] and will later be used to compare the SOI microdosimeter data.

C. Microdosimeter Test Setup

The SOI microdosimeter system was developed by the Centre for Medical Radiation Physics (CMRP) at the University of Wollongong, Australia [27]. The setup is shown in Fig. 2 which also shows the Si diodes used for standard dosimetry in the facility and two commercial static random access memorys (SRAMs) used for SEU testing placed on the same frame. The microdosimeter device is mounted on the MicroPlus probe which is enclosed in a PMMA sheath wrapped in aluminum. The probe was connected to a shaping amplifier through which the bias supply to the device was provided from a portable battery box. The shaper was also electrically connected to the support to reduce signal noise. The readout signal was fed through a 2 m coaxial cable to an Amptek MCA8000D pocket multi-channel analyzer (MCA) with live acquisition of energy deposition spectra using the Amptek MCA desktop software DppMCA. The spectra were analyzed using the CMRP microdosimetry suite software, converting from energy deposition spectra to lineal energy distributions and calculating their microdosimetric quantities. During this test campaign, several different microdosimeters (SV diameters of 20 μm and thickness of 5 [8] and 10 μm [28]) were tested with different gains (high, medium, and low, respectively). The 5 μm device contained 400 SVs, whereas the 10 μm device contained 1600 SVs. Both were calibrated at CMRP using a pulse generator and 5.48 MeV alpha particles. At each configuration change, a noise check using an oscilloscope was carried out.

IV. SOI Microdosimeter Measurement Results

During each acquisition period, the signal threshold was chosen to cut off noise-level events or energy deposition events due to very light fragments with low LET or particle flux was adjusted to reduce pile-up. Particle fluxes for all measurements were chosen such that there is no pile-up and ranged between 10^3 and 10^4 ions/cm^2/s averaged over a 350 μs spill duration. For each DUT, the three primary extracted energies, 650, 750, and 1000 MeV/n, either with or without the use of degraders. Example energy spectra are shown at the top of Fig. 3. At the bottom of the same figure, the conversion to standard microdosimetric lineal energy spectra is made, showing the characteristic double lobe distribution of low-y events caused by light secondary particles and noise, and a high-y peak caused by the primary beam particles. Analysis of these spectra revealed that only measurements made at low gain (dynamic range up to an energy of 176 MeV) could register all energy deposition events for each experimental configuration. Since for all measurements, the beam was oriented in a perpendicular way to the device, it is assumed that the average chord length is equal to the height of the SVs, that is, 5 and 10 μm, respectively [29].

TABLE I
OVERVIEW OF MEASUREMENT RESULTS CORRESPONDING TO A SIMILAR LET

Energy [MeV/n]	Degrader thickness [mm]	Device	$\bar{y}_{\mathrm{fit}}$ (FWHM) [10^3 keV/μm]	$\mathrm{LET}_{\mathrm{fit}}$ (FWHM) [MeVcm^2/mg]	$\mathrm{LET}_{\mathrm{FLUKA}}$ (FWHM) [MeVcm^2/mg]
750		5um, low	3.33 (0.53)	14.3 (2.3)	17.5 (0.5)
		10um, low	2.97 (0.37)	12.7 (1.6)	
1000	30	5um, low	3.50 (0.85)	15.0 (3.6)	
750	10	5um, low	4.50 (0.87)	19.3 (3.7)	21.5 (1.2)
1000	38	5um, low	4.76 (1.03)	20.4 (4.4)	

Starting from 1000 MeV/n (reduced down to 660 MeV/n at the test location), the LET booster system was used to carry out a Bragg peak-like scan of deposited energy as a function of degrader thickness. This is shown in Fig. 4 by plotting $\bar{y}_D$ as a function of the cumulative PMMA degrader thickness using data from the 5 and 10 μm devices at low gain. For 0, 30, 42, and 50 mm thickness also the energy deposition and microdosimetric spectra are shown. The energy deposition spectra were fit with a Gaussian function extracting the mean value and full width at half maximum (FWHM). These were converted to LET values in silicon and shown on the bottom right of Fig. 4. For reference, the results from using the stopping and range of ions in matter (SRIM)-based StackUp tool developed by NSRL [30] (v9) are also shown. The StackUp tool is more limited in capabilities, allowing only to use of a Pb ion beam at a fixed 660 MeV/n energy and 1-D materials, whereas the other simulations described in this work use a dispersed and fragmented beam in a more realistic geometry. For degrader thicknesses below 30 mm, the agreement with the other methods is good; however, closer to the Bragg peak the values diverge drastically, reaching a nearly 50% underestimation of the LET with respect to the microdosimetric y_{fit} value at 42 mm cumulative degrader thickness. Experimental configurations which yield a similar LET were determined by Monte Carlo simulations benchmarked against solid state detector measurements. These are shown in Fig. 5 and Table I for two LET values: 17.5 and 21.5 MeV $\cdot$ cm^2/mg as extracted from FLUKA simulations. Differences in results obtained from the 5 and 10 μm devices for the same beam energy could be due to a different SV thickness in reality or calibration inconsistencies.

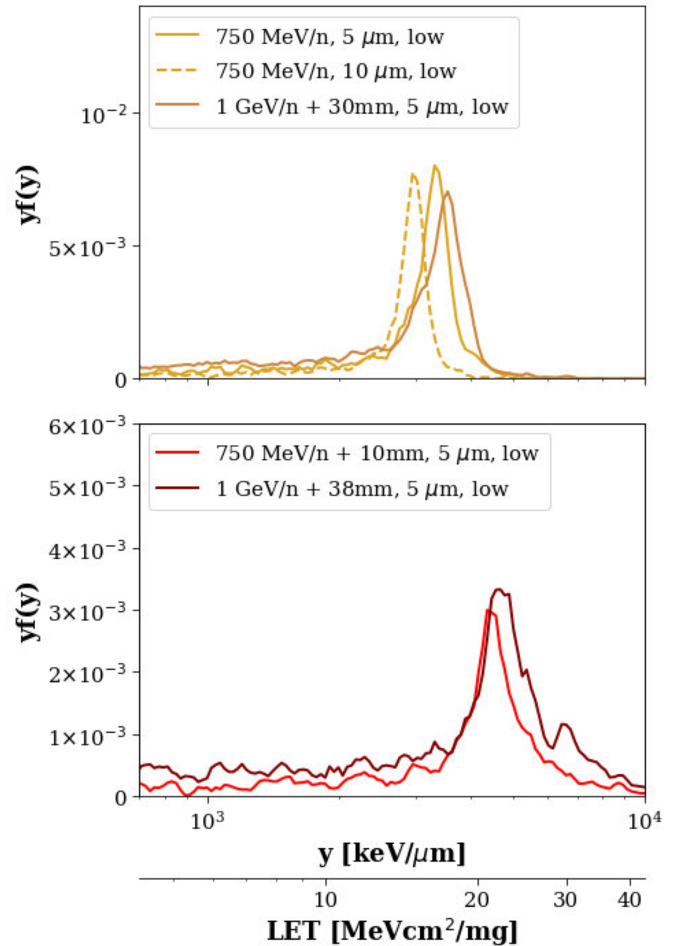

Fig. 5. Microdosimetric spectra of different beam and PMMA degrader configurations. The top and bottom subplots correspond to configurations that result in a beam LET of 17.5 and 21.5 MeV $\cdot$ cm^2/mg.

V. DISCUSSION

As shown in Fig. 3, the simulated detector response from FLUKA shows an excellent agreement with measurements for the three main primary energies, verifying the adequacy of the geometric model and simulation of interactions on a microscopic level. This very same simulation model yields the LET values used in the "classic" dosimetry method using benchmarked Si diode energy deposition spectra. The quantities standardly used in a radiobiology context $\bar{y}_F$ and $\bar{y}_D$ are not readily applicable in the context of microelectronics SEE testing. Nevertheless, the sensitivity to increasing degrader thickness is observed largely as expected as shown in Fig. 4 (bottom left). Before the Bragg peak is reached, a clear peak in the spectrum is shown corresponding to events caused by the primary beam particles. At and beyond the Bragg peak, the spectrum no longer exhibits a clear peak and VHE events are acquired as shown in Fig. 4 (top row). When converted to silicon LETs, the mean values from the fit lineal energy deposition spectra show a reasonable agreement with

the LET values extracted from FLUKA simulations, lying within 20% in relative terms except for the value closest to the Bragg peak showing a difference of nearly 10 MeV $\cdot$ cm^2/mg. When approaching the Bragg peak above a cumulative degrader thickness of 40 mm, it is to be noted that the FWHM spread on the microdosimetric energy deposition distribution becomes 2–3 times larger than that predicted by the LET distributions from FLUKA. The width of these distributions is a combination of the beam energy spread and the spread of the event energy deposition. The comparable LET configurations shown in Fig. 5 and Table I exhibit a reasonable agreement to the simulation-predicted LETs as well albeit being lower in all cases; for the 21.5 MeV $\cdot$ cm^2/mg configurations all values even agree within 10%. Again here, the spread on LET values obtained from microdosimetry is at least a factor of two larger than those predicted by simulations.

VI. Conclusion

Microdosimetry using SOI detector devices was demonstrated for characterizing VHE Pb ion beams dedicated to SEE testing. Using key microdosimetric quantities, the effect of using passive energy degraders on the resulting linear energy spectrum was observed, boosting the resulting radiation field to higher deposited energies. The use of the standard lineal energy spectrum moments ($\bar{y}_F$, $\bar{y}_D$) showed limited applicability in the microelectronics SEE testing context; the spectra themselves could, however, yield important information on the frequency of low energy deposition events which can be of importance when testing sensitive devices in a mixed-field environment. The average lineal energies when converted to LET in Si showed reasonable agreement with the values extracted from benchmarked MC simulations in FLUKA, where differences could arise due to non-uniformity of the SVs (the SOI wafer manufacturer allows a 5% non-uniformity of the 5 μm active layer). With respect to the classical dosimetry approach, which requires these simulations to extract the LET, microdosimetry directly shows the deposited energy in a stochastic way rather than showing the deterministic energy loss. The microdosimetric spectra yield a more direct, experimental view of high energy deposition events in a more representative size of volume for microelectronics. Dosimetry on the nanometer level can be worth exploring given the nm length scale of sensitive nodes in current electronic technologies.

References

[1] R. G. Alía et al., "Heavy ion energy deposition and SEE intercomparison within the RADNEXT irradiation facility network," *IEEE Trans. Nucl. Sci.*, vol. 70, no. 8, pp. 1596–1605, Mar. 2023.

[2] K. Bilko et al., "CHARM high-energy ions for microelectronics reliability assurance (CHIMERA)," *IEEE Trans. Nucl. Sci.*, vol. 71, no. 8, pp. 1549–1556, Aug. 2024.

[3] R. G. Alía et al., "The HEARTS EU project and its initial results on fragmented high-energy heavy ion single event effects testing," *IEEE Trans. Nucl. Sci.*, early access, Jan. 16, 2025, doi: 10.1109/TNS.2025.3530502.

[4] C. Zeitlin, S. B. Guetersloh, L. H. Heilbronn, and J. Miller, "Measurements of materials shielding properties with 1 GeV/nuc ^{56}Fe," *Nucl. Instrum. Methods Phys. Res. Sect. B, Beam Interact. Mater. At.*, vol. 252, no. 2, pp. 308–318, Nov. 2006.

[5] A. Wroe et al., "Solid state microdosimetry with heavy ions for space applications," *IEEE Trans. Nucl. Sci.*, vol. 54, no. 6, pp. 2264–2271, Dec. 2007.

[6] S. N. Ahmed, "Dosimetry and radiation protection," in *Physics and Engineering of Radiation Detection*, 2nd ed., S. N. Ahmed, Ed., Amsterdam, The Netherlands: Elsevier, 2015, pp. 621–688.

[7] Y. Chiang, C. M. Tan, C.-J. Tung, C.-C. Lee, and T.-C. Chao, "Lineal energy of proton in silicon by a microdosimetry simulation," *Appl. Sci.*, vol. 11, no. 3, Feb. 2021, Art. no. 1113.

[8] B. James et al., "SOI thin microdosimeters for high LET single-event upset studies in Fe, O, Xe, and cocktail ion beam fields," *IEEE Trans. Nucl. Sci.*, vol. 67, no. 1, pp. 146–153, Jan. 2020.

[9] J. F. Dicello, "Microelectronics and microdosimetry," *Nucl. Instrum. Methods Phys. Res. Sect. B, Beam Interact. Mater. At.*, vols. 24–25, pp. 1044–1049, Apr. 1987.

[10] S. Peracchi et al., "LET calibration of ion microbeams and their SEE cross section characterization," *IEEE Trans. Nucl. Sci.*, vol. 71, no. 8, pp. 1565–1570, Aug. 2024.

[11] C. Ahdida et al., "New capabilities of the FLUKA multi-purpose code," *Frontiers Phys.*, vol. 9, Jan. 2022, Art. no. 788253.

[12] G. Battistoni et al., "Overview of the FLUKA code," *Ann. Nucl. Energy*, vol. 82, pp. 10–18, Aug. 2015.

[13] A. Waets et al., "Very-high-energy heavy ion beam dosimetry using solid state detectors for electronics testing," *IEEE Trans. Nucl. Sci.*, vol. 71, no. 8, pp. 1837–1845, Aug. 2024.

[14] N. Emriskova, A. Waets, O. D. L. R. Du, K. Klimek, and R. G. Alía, "Characterisation of degraded very-high-energy heavy ion beams using the HEARTS LET booster," *IEEE Trans. Nucl. Sci.*, early access, Jan. 10, 2025, doi: 10.1109/TNS.2024.3521185.

[15] P. D. Bradley, A. B. Rosenfeld, and M. Zaider, "Solid state microdosimetry," *Nucl. Instrum. Meth. Phys. Res. B, Beam Interact. Mater. At.*, vol. 184, no. 1, pp. 135–157, Sep. 2001.

[16] A. B. Rosenfeld, "Novel detectors for silicon based microdosimetry, their concepts and applications," *Nucl. Instrum. Methods Phys. Res. A, Accel. Spectrom. Detect. Assoc. Equip.*, vol. 809, pp. 156–170, Feb. 2016.

[17] A. M. Kellerer, "Fundamentals of microdosimetry," in *The Dosimetry of Ionizing Radiation*, K. R. Kase, Ed., Orlando, FL, USA: Academic Press, 1985, pp. 77–162.

[18] G. A. S. Cruz, "Microdosimetry: Principles and applications," *Rep. Practical Oncol. Radiotherapy*, vol. 21, no. 2, pp. 135–139, Apr. 2016.

[19] H. H. Rossi and M. Zaider, *Microdosimetry and Its Applications*. Berlin, Germany: Springer, 1996.

[20] E. Johnson et al., "Beam optics modelling of slow-extracted very high-energy heavy ions from the CERN proton synchrotron for radiation effects testing," in *Proc. 15th Int. Part. Accel. Conf. (IPAC)*, 2024, pp. 3560–3563.

[21] A. Thornton. (2016). *CHARM Facility Test Area Radiation Field Description*. [Online]. Available: https://cds.cern.ch/record/2149417

[22] A. Waets et al., "Heavy ion beam characterization for radiation effects testing at CERN using Monte Carlo simulations and experimental benchmarking," in *Proc. 14th Int. Part. Accel. Conf.* Geneva, Switzerland: JACoW, May 2023, pp. 5106–5109.

[23] H. H. Braun, A. Fassò, A. Ferrari, J. M. Jowett, P. R. Sala, and G. I. Smirnov, "Hadronic and electromagnetic fragmentation of ultrarelativistic heavy ions at LHC," *Phys. Rev. Special Topics-Accel. Beams*, vol. 17, no. 2, Feb. 2014, Art. no. 021006.

[24] G. Battistoni et al., "The FLUKA code: Description and benchmarking," in *Proc. AIP Conf.*, Mar. 2007, pp. 31–49.

[25] A. Lechner, "Particle interactions with matter," in *Proc. CERN Yellow Rep. School*, Dec. 2018, pp. 47–67.

[26] K. S. Krane, *Introductory Nuclear Physics*. New York, NY, USA: Wiley, 1988.

[27] L. T. Tran et al., "Silicon 3D microdosimeters for advanced quality assurance in particle therapy," *Appl. Sci.*, vol. 12, no. 1, Dec. 2022, Art. no. 328.

[28] B. James et al., "SOI thin microdosimeter detectors for low-energy ions and radiation damage studies," *IEEE Trans. Nucl. Sci.*, vol. 66, no. 1, pp. 320–326, Jan. 2019.

[29] A. T. Samnøy et al., "Microdosimetry with a 3D silicon on insulator (SOI) detector in a low energy proton beamline," *Radiat. Phys. Chem.*, vol. 176, Nov. 2020, Art. no. 109078.

[30] *NSRL StackUp Tool (V9)*. Brookhaven Nat. Lab., Upton, NY, USA. Accessed: Aug. 9, 2024. [Online]. Available: https://www.bnl.gov/nsrl/stackup/